Problem Set 1

1. (4 points) The cosmic microwave background (CMB) radiation has a nearly perfect blackbody spectrum with temperature $T \approx 2.73$ K. In the low-frequency limit, calculate the slope of the CMB curve as plotted in the figure below (*ERA* Figure 1.4).

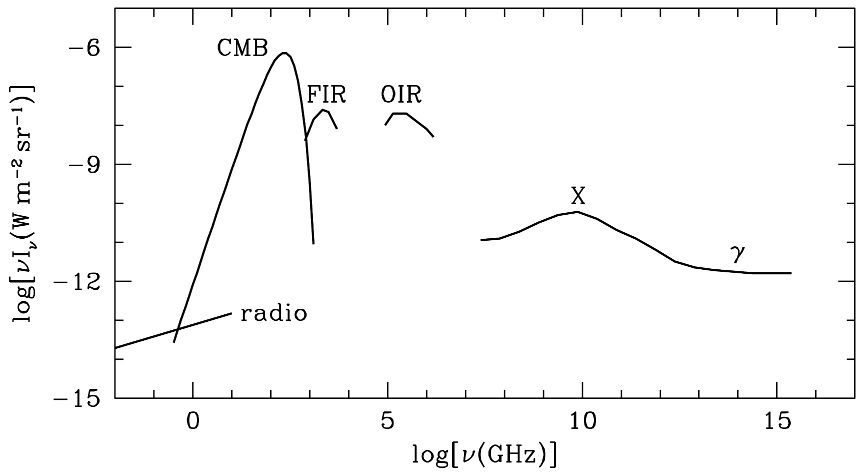

2. (4 points) The "radio" background is produced by radio sources having power-law spectra of the form

$$S_\nu \propto \nu^\alpha$$

where the exponent α is called the spectral index. For the typical radio-source spectral index $\alpha \approx -0.7$, calculate what the slope of the "radio" line should be in *ERA* Figure 1.4.

3. (4 points) In 1903 the Einwegspiegel Mirror Company of Bern, Switzerland submitted a patent application for a one-way mirror for use by psychologists who wanted to observe their subjects without being seen themselves. The application stated that the one-way mirror had different special coatings on sides "a" and "b" such that light going from side "a" to side "b" went through the mirror more easily than light going from side "b" to side "a". The application was rejected by patent clerk A. Einstein. Why?

4. (8 points) At its closest approach on July 28, 2018, the planet Mars:
(1) was $d \approx 5.8 \times 10^7$ km from the Earth,
(2) its angular diameter was $\theta \approx 25$ arcsec, and
(3) its $\nu = 1.4$ GHz flux density was $S \approx 0.14$ Jy.

   a. (3 points) What was the Rayleigh-Jeans brightness temperature T_b of Mars at $\nu = 1.4$ GHz?

   b. (3 points) The 1.4 GHz radar reflectivity of Mars is $r \approx 0.1$. If Mars is a purely thermal source, what is the physical temperature T of Mars?

   c. (2 points) Which of the three pieces of information given above wasn't needed to answer parts (a) and (b) of this question?

Problem Set 2

5. (4 points) One definition of the "habitable zone" around a star is the region in which liquid water could exist on a planet. Estimate the inner and outer radii $r_{\rm in}$ and $r_{\rm out}$ of the habitable zone around the Sun by calculating the distance from the Sun at which the radiative equilibrium temperature of an *isothermal* black body is the boiling temperature of water ($T_{\rm in} \approx 100$ C ≈ 373 K) and the distance at which water freezes ($T_{\rm out} \approx 0$ C ≈ 273 K). (To be nearly isothermal, an actual planet or asteroid would have to be spinning fast enough and/or have enough atmosphere that its daytime and nighttime temperatures are nearly equal.) Express $r_{\rm in}$ and $r_{\rm out}$ in units of "astronomical units" (AU), where 1 AU $\approx 1.496 \times 10^{13}$ cm is defined as the mean radius of the Earth's orbit around the Sun.

6. (4 points) The Rayleigh-Jeans brightness temperature $T_{\rm b}$ defined by *ERA* Equation 2.33 is close to the physical temperature T of a blackbody source only in the low-frequency limit $\nu \ll h/(kT)$. Calculate the ratios $(T_{\rm b}/T)$ for the $T = 2.73$ K cosmic microwave background (CMB) at frequencies $\nu = 1$, 10, 100, and 1000 GHz.

7. (6 points) The classical Larmor's formula (*ERA* Equation 2.143) for radiation from an accelerated charged particle implies that the electron orbiting the proton in a hydrogen atom will radiate away its kinetic energy in a small fraction of a second, and the atom will collapse. This striking failure was one of the problems in classical physics that led to the development of quantum mechanics. A classical hydrogen atom consists of an electron in a circular orbit around a proton, with the centrifugal force $m_{\rm e} v_{\rm e}^2 / r_0$ balancing the Coulomb force e^2/r_0^2. Here $r_0 = 5.3 \times 10^{-9}$ cm is the orbital radius, called the Bohr radius. The classical radiative lifetime t of such an atom is the electron kinetic energy E divided by the Larmor power radiated when $r = r_0$. Estimate t.

8. (6 points) As a plane wave of electromagnetic radiation passes a free charged particle initially at rest, the electric field E of that radiation will accelerate the particle, which in turn will radiate power in all directions according to Larmor's equation. This process is called scattering rather than absorption because the total power in electromagnetic radiation is unchanged—all of the power extracted from the incident plane wave is reradiated in other directions. For a free electron of charge e and mass $m_{\rm e}$, the geometric area that would intercept this amount of scattered power from the incident plane wave is called the Thomson scattering cross section $\sigma_{\rm T}$. Derive *ERA* Equation 5.33 for $\sigma_{\rm T}$:

$$\sigma_{\rm T} = \frac{8\pi}{3}\left(\frac{e^2}{m_{\rm e} c^2}\right)^2 .$$

Problem Set 3

9. Many of the Fourier transform theorems in *ERA* Appendix A.6 can be derived easily, starting from the definition of the Fourier transform $F(s)$ of the function $f(x)$ (*ERA* Equation A.1):

$$F(s) \equiv \int_{-\infty}^{\infty} f(x) e^{-2\pi i s x} dx \ .$$

For example, the **addition theorem** (*ERA* Equation A.1) for the Fourier transform $H(s)$ of the sum $h(x) = f(x) + g(x)$ is simply

$$\begin{aligned} H(s) &= \int_{-\infty}^{\infty} [f(x) + g(x)] e^{-2\pi i s x} dx \\ H(s) &= \int_{-\infty}^{\infty} f(x) e^{-2\pi i s x} dx + \int_{-\infty}^{\infty} g(x) e^{-2\pi i s x} dx \\ H(s) &= F(s) + G(s) \ , \end{aligned}$$

which can be written compactly as

$$f(x) + g(x) \leftrightarrow F(s) + G(s) \ .$$

Two Fourier transform theorems are especially important for radio astronomy—the **similarity theorem** and the **modulation theorem**.

(a) (3 points) Derive the similarity theorem (*ERA* Equation A.11)

$$f(ax) \leftrightarrow \frac{F(s/a)}{|a|} \ ,$$

where a is a constant scaling factor. The similarity theorem is used in *ERA* Section 3.2.4 to show that the angular beamwidth of an aperture antenna is inversely proportional to the aperture diameter in wavelengths, D/λ. The bigger the aperture, the narrower the beam.

(b) (3 points) Derive the modulation theorem (*ERA* Equation A.12)

$$f(x)\cos(2\pi\nu x) \leftrightarrow \frac{1}{2}F(s-\nu) + \frac{1}{2}F(s+\nu) \ .$$

The modulation theorem is the basis of the ubiquitous superheterodyne receiver (*ERA* Section 3.6.4 and Figure 3.39). Let the variable x be time t, so the complementary variable s is frequency ν. In a superheterodyne receiver the input radio-frequency signal $f(t)$ is multiplied in a mixer by a monochromatic local oscillator signal $\cos(2\pi\nu_{\mathrm{LO}}t)$ at frequency ν_{LO}. The result is that input radio-frequency signals at frequency ν_{RF} are shifted in frequency to the intermediate frequencies $\nu_{\mathrm{IF}} = \nu_{\mathrm{RF}} - \nu_{\mathrm{LO}}$ and $\nu_{\mathrm{IF}} = \nu_{\mathrm{RF}} + \nu_{\mathrm{LO}}$. For example, a local oscillator at $\nu_{\mathrm{LO}} = 12$ GHz can be used to shift an input radio signal at frequency $\nu_{\mathrm{RF}} = 9$ GHz down to a lower frequency $\nu_{\mathrm{IF}} = 3$ GHz where it is easier to process.

Hint: Rewrite $\cos(2\pi\nu x)$ as a complex exponential (see *ERA* Appendix B.3).

10. This question involves performing some image processing using 2-D Fourier Transforms. As for the last problem set, you will need to use data analysis software like *Matlab*, *IDL*, *Mathematica*, or (recommended) a scientific install of *Python*. Please plot all images in greyscale.

(a) (2 points) *Black and White Image of You*
Your first task is to take a headshot picture of yourself with your phone or laptop and to save it as a greyscale image at a size of 512x512 pixels. That image will be the basis of your Fourier image processing experiments. (Note: make sure that you have a true greyscale image and not one with RGB channels adjusted to appear as greyscale). Show your image.

(b) (4 points) *Amplitudes and Phases*
Load your image into your analysis software along with the image of trees found here:
`http://www.cv.nrao.edu/~sransom/trees.jpg`
Take the Fourier transforms of each image. Calculate the Fourier amplitudes and phases for each of the transforms. (Note: make sure that you compute the phases correctly so that they can have values over 2π radians!) Now make two new images where you combine the Fourier amplitudes from one of the input images with the Fourier phases from the other input image. Show the image that looks most like you. Does that image contain the amplitudes or the phases from the original image of you?

(c) (4 points) *Image Filtering I*
Set the amplitudes of all Fourier frequencies ≤ 20 in the FFT of your image equal to zero. Inverse FFT and make a new image. (Hint: Be very careful choosing which parts of the Fourier array to set to zero. The layout of these arrays is implementation dependent. Plotting the log of the Fourier amplitudes will help. Also remember that there are negative Fourier frequencies!) What type of filter did you just apply? What parts of the image are accentuated? Plot both the log of the filtered Fourier amplitudes as well as the new image.

(d) (4 points) *Image Filtering II*
Set the amplitudes of all Fourier frequencies > 20 in the FFT of your image equal to zero. Inverse FFT and make a new image. What type of filter did you just apply? What causes the excess ripples or ringing in the resulting image and how might you mitigate that? Plot both the log of the filtered Fourier amplitudes as well as the new image.

(e) (4 points) *Convolution*
Make a two-dimensional symmetric gaussian kernel of FWHM 20 pixels with which to smooth your image. Then perform the smoothing via FFT using the convolution theorem. (Hint: given the nature of how FFTs are computed, you may need to re-position your kernel in its input array so that you get a "nice" output image. Most analysis languages have a special function to do this for you, for instance `fftshift` in *Matlab* and *Numpy*.) Plot the kernel and the resulting smoothed image.

Problem Set 4

11. (6 points) *ERA* Equation 3.60 relates the height z of a paraboloidal reflector to the distance r from the symmetry axis and the focal length f:

$$z = \frac{r^2}{4f}$$

This equation was derived from the requirement that all parts of wave fronts traveling parallel to the z axis must go the same distance to reach the focus at $z = f$ (*ERA* Figure 3.7).

Alternatively, the equation for a paraboloidal reflector can be derived from the requirement that, for any mirror, the angle of incidence $\theta_{\rm i}$ equals the angle of reflection $\theta_{\rm r}$. The figure below shows the incoming ray as a vertical dashed line, the reflected ray as the dashed line going to the focus, and the mirror normal as the solid line between them.

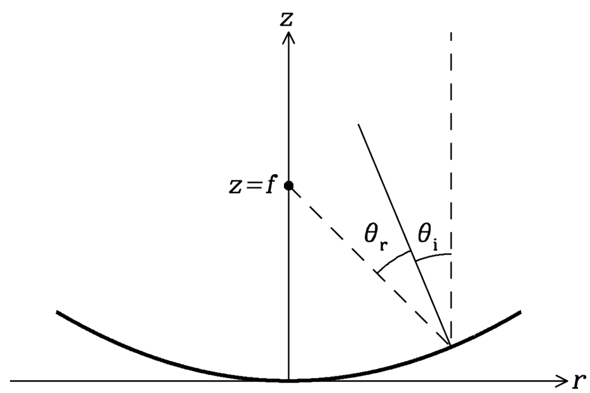

Use $\theta_{\rm i} = \theta_{\rm r}$ to confirm that a parabola with $z = r^2/4f$ will focus the incoming rays onto the point $z = f$, $r = 0$.

12. (4 points) Using the fact that a dipole antenna can transmit or receive only linearly polarized radiation whose $\vec{E}$ vector is parallel to the dipole, show that equilibrium radiation cannot be linearly polarized.

13. (4 points) In 1903 the Doppel Dipol Antenne Company of Bern, Switzerland submitted a patent application for their new "double dipole" antenna system that could collect all of the incident power from both horizontal and linear polarizations simultaneously. Unlike the usual crossed dipoles with separate two-terminal outputs, a black box in the Doppel Dipol system combines both polarizations using a secret method to send double the power to a single two-terminal output when fed by an unpolarized signal. The application was rejected by patent clerk A. Einstein. Why?

14. (6 points) *ERA* Figure 3.7 shows the parabolic cross section of a paraboloidal dish of the type used in radio astronomy. The dish reflects plane waves from a distant source onto the focal point labeled f, where a small feed antenna collects the radiation. (The term "feed" used by radio astronomers is actually more appropriate for a transmitting antenna whose feed transmits power onto ("illuminates") the dish, which focuses the power into a narrow beam.)

A horizontal dipole antenna could be used as a feed, but it would be very inefficient because its power pattern is nearly isotropic (in fact, it is isotropic in the plane normal to the dipole arms), so less than half of the power transmitted by a dipole feed actually intercepts the dish. To improve the performance of a dipole feed, radio astronomers put a flat mirror 1/4 wavelength behind the dipole to create a virtual antenna 1/4 wavelength behind the flat mirror, as shown in the figure below.

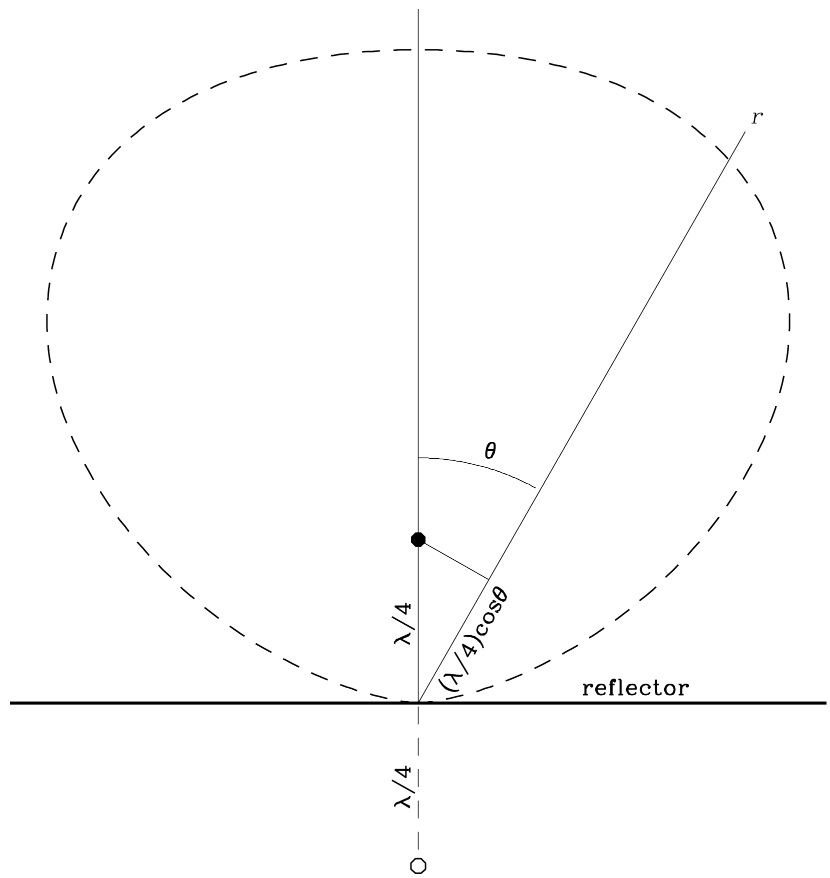

The real end-on horizontal dipole is indicated by the filled circle, and the mirror-image dipole by the open circle below the reflector.

At large distances $r \gg \lambda$ from the feed, the angle θ between the normal to the mirror and a ray is very nearly the same for both the real and image dipoles. Rays from the image dipole must travel a distance $d = 2(\lambda/4)\cos\theta$ farther than those from the real dipole, causing a geometric phase delay of $d(2\pi/\lambda)$ radians. In addition, reflection changes the image antenna phase by $180^\circ = \pi$ radians, so the total phase difference between the real and image antennas is

$$\phi = \frac{2\pi\lambda\cos\theta}{2\lambda} - \pi = \pi\cos\theta - \pi$$

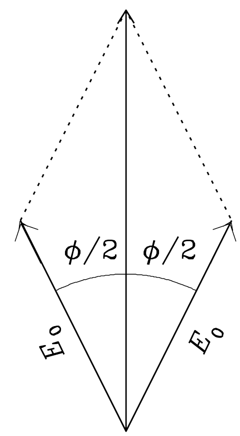

The total radiated electric field from this system is the vector sum of the electric fields of the real and image antennas. If the real and image isotropic antennas both produce electric fields of amplitude E_0 at $r \gg \lambda$, show by trigonometry that the vector sum of their electric fields has amplitude

$$E = 2E_0 \sin\left(\frac{\pi}{2}\cos\theta\right) \quad \text{for} \quad |\theta| < \pi/2.$$

The corresponding power pattern is proportional to E^2; it is shown as the dashed curve in the figure. No power is wasted by going behind the reflector ($|\theta| > \pi/2$), and the power in front of the reflector is concentrated in a beam of width ≈ 2 radians, which is just about the right width to illuminate a parabolic reflector like the one shown in *ERA* Figure 3.7.

This problem isn't just a theoretical exercise; the actual low-frequency ($\nu \lesssim 1$ GHz) feeds used at the Green Bank Telescope (GBT) are crossed dipoles (to receive both linear polarizations) $\lambda/4$ in front of flat reflecting disks. The photo below shows the GBT's 290–395 MHz ($\lambda \approx 0.9$ m) crossed-dipole feed.

Problem Set 5

15. (10 points) The GBT has an unblocked circular aperture 100 m in diameter, and its aperture efficiency is $\eta_{\rm A} \approx 0.70$ at low frequencies. The rms error in the GBT surface is $\sigma \approx 0.21$ mm.
    (a) (4 points) Estimate the aperture efficiency of the GBT at $\nu = 45$ GHz.
    (b) (4 points) The GBT is pointed at the unresolved and unpolarized calibration source 3C 295, whose 45 GHz flux density is $S_\nu = 0.39$ Jy. Neglecting atmospheric absorption, estimate the antenna temperature added by 3C 295.
    (c) (2 points) Estimate the half-power beamwidth $\theta_{\rm HPBW}$ in arcsec of the GBT at 45 GHz.

16. (4 points) *ERA* Equation 3.133
$$\lambda = 4\pi\sigma$$
gives the wavelength λ at which the gain of a reflector antenna with rms surface error σ is highest. Derive this equation.

17. (2 points) The traditional requirement on the rms pointing accuracy of a telescope is $\sigma \approx \theta_{\rm HPBW}/10$. If the telescope is mis-pointed by this amount, was is the fractional loss of gain?

18. (4 points) For large telescopes like the GBT, high-frequency performance is limited by pointing as well as by surface accuracy.
    (a) What is the required rms GBT pointing accuracy σ at $\nu = 45$ GHz, expressed in radians?
    (b) Compare this with the thermal expansion coefficient of steel, which is about 12 parts per million per Centigrade degree. Estimate the maximum tolerable temperature differential across the telescope when observing at 45 GHz.

You would like to use the VLA at $\nu = 6$ GHz to make a continuum image of a planetary nebula that is a nearly uniform circular disk with angular diameter $\phi \approx 10$ arcsec and total flux density $S_\nu \approx 10$ mJy.

19. (4 points) What is the brightness temperature T_b of the planetary nebula at $\nu = 6$ GHz?

20. (12 points) The VLA exposure calculator at `https://obs.vla.nrao.edu/ect/` can be used to calculate the on-source observing time needed to reach a given sensitivity. Results from the exposure calculator must be included in any VLA observing proposal to show that the proposed observations are feasible.

   (a) (4 points) At `https://obs.vla.nrao.edu/ect/` set the *Representative Frequency* to 6.0 GHz and the *Bandwidth* to 4.0 GHz, the maximum available bandwidth at this frequency. You should get a warning about "Severe RFI effects" noting that 15% of the band may be obliterated by RFI. The screen should look like the figure below:

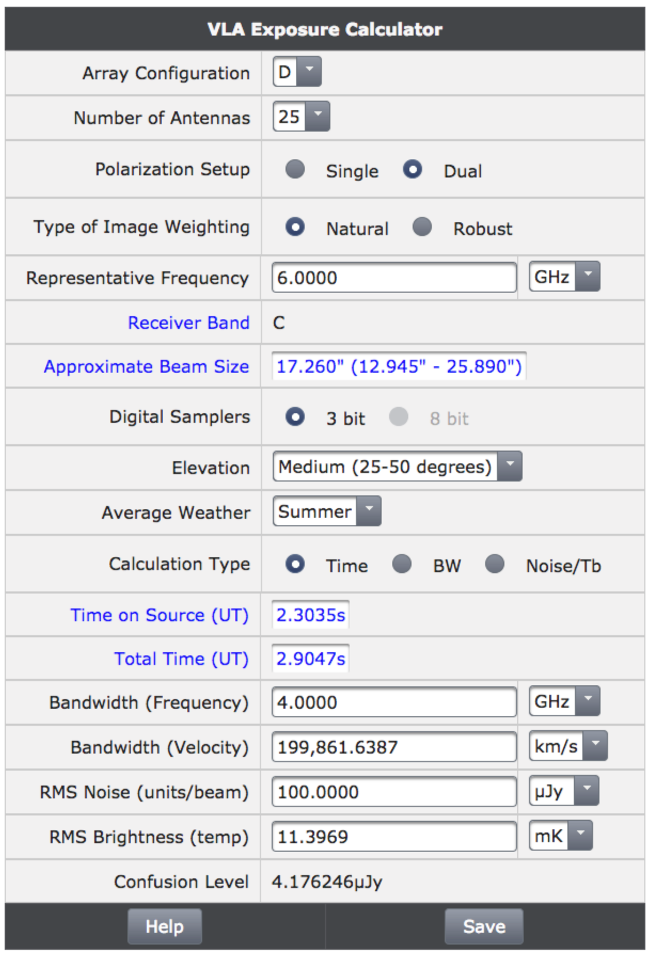

   The VLA is centrally concentrated, so *Natural* weighting gives a poor beam shape. Select *Robust* image weighting that assigns more weight to the longer baselines and notice that the *Approximate Beam Size* shrinks to $\theta \approx 12$ arcsec. Use this result to estimate the effective diameter of the VLA D Configuration with *Robust* weighting.

   (b) (2 points) Change the *Array Configuration* from D to A. With *Robust* weighting, the beam size should now be $\theta \approx 0.326$ arcsec. What is the effective size of the A configuration with *Robust* weighting?

(c) (4 points) To allow for frequency ranges lost to RFI, reduce the *Bandwidth* to 3.4 GHz. For the default *RMS Noise* $= 100\,\mu$Jy beam^{-1}, what is the required *Time on Source* and how does it change when going from the A to B to C configurations? Why?

(d) (2 points) Keeping the default *RMS Noise* $= 100\,\mu$Jy beam^{-1}, what the *RMS Brightness (temp)* noise in the A, B, C, and D configurations? For which configurations is the *RMS Brightness (temp)* noise less than 1/5 of the source brightness temperature?

21. (4 points) You would like to observe the planetary nebula with enough brightness sensitivity to get a brightness signal-to-noise ratio SNR $\equiv T_{\rm b}/\sigma_T \geq 50$. How much *Time on Source* is needed in the D, C, B, and A configurations? Why do these times vary so much (each successive time is $\approx 100\times$ the time required for the next smaller array)?

Problem Set 7

22. (6 points) Consider an east-west two-element interferometer like the one shown in *ERA* Figure 3.41, with a baseline length $b = 1$ km operating at $\nu = 6$ GHz.

    (a) (4 points) For a radio star on the celestial equator observed near transit, what is the "natural" fringe frequency $\nu_{\rm f}$ (Hz) caused by the Earth's rotation?

    (b) (2 points) What is the natural fringe frequency for a source at the north celestial pole?

23. (6 points) *ERA* Equation 3.203 gives the rms noise in units of point-source flux density for an interferometer image made with natural weighting, a single polarization, and a perfect analog correlator:

$$\sigma_S = \frac{2kT_{\rm s}}{A_{\rm e}[N(N-1)\Delta\nu\,\tau]^{1/2}} \ .$$

Here $T_{\rm s}$ is the system noise temperature, $A_{\rm e}$ is the effective collecting area of each antenna, N is the number of antennas in the array, $\Delta\nu$ is the bandwidth, and τ is the on-source integration time. Most VLA observations use two polarizations ($n_{\rm pol} = 2$), and the VLA correlator efficiency with 8-bit samplers is only $\eta_{\rm c} \approx 0.93$. Thus a better estimate of the rms noise in a naturally weighted VLA image is

$$\sigma_S = \frac{2kT_{\rm s}}{\eta_{\rm c}\,A_{\rm e}[n_{\rm pol}\,N(N-1)\Delta\nu\,\tau]^{1/2}} \ .$$

The VLA consists of $N = 27$ $D = 25$ m antennas, of which $N = 25$ are typically working, so the VLA on-line exposure calculator (`https://obs.vla.nrao.edu/ect`) uses $N = 25$ as the default. At S band ($\nu = 3$ GHz), the VLA system noise temperature is about 40 K and the aperture efficiency is $\eta_{\rm a} \approx 0.62$. The bandwidth of the receiver is 2 GHz, but RFI limits its maximum usable bandwidth to $\Delta\nu \approx 1.5$ GHz. Using these parameters, estimate how much on-source integration time τ would be needed to reach an rms noise $\sigma_S = 10\,\mu$Jy beam^{-1}.

24. (8 points) The VLA exposure calculator at `https://obs.vla.nrao.edu/ect` helps astronomers proposing for telescope time to estimate their required on-source observing times τ.

    Use that calculator to verify your result from the previous problem. Set the *Array Configuration* to A to make sure the *Confusion Level* is zero and use the defaults *Elevation* = medium and *Average Weather* = Summer.

    (a) (4 points) Convert the VLA result for *Time on Source (UT)* to seconds. What value did you get? [Note: It should equal within a few percent the result you calculated for the previous problem. If so, congratulations! You know more about calculating sensitivities than many NRAO users. If not, check that all of the input fields for the VLA Exposure Calculator are correct and/or recheck your calculation for the previous problem until you get agreement.]

    (b) (4 points) Change the Array Configuration from A (maximum baseline ≈ 35 km) to B (maximum baseline ≈ 11 km). The required *Time on Source (UT)* should not change because the rms confusion in both configurations is much less than $10\,\mu$Jy beam^{-1}. Next change the Array Configuration from B to C (maximum baseline ≈ 3 km). Notice that the required *Time on Source* has increased slightly. Although the VLA system noise hasn't changed, the rms confusion has increased by an order-of-magnitude to $\sigma_{\rm c} \approx 2.44\,\mu$Jy beam^{-1} because the C-array beam area is about $10\times$ larger than the B-array beam area. The total image variance σ^2 is the sum of the statistically independent noise variance σ_S^2 and confusion variance σ_c^2:

$$\sigma^2 = \sigma_S^2 + \sigma_{\rm c}^2 \ .$$

    Calculate the value of σ_S needed to keep the image RMS $\sigma = 10\,\mu$Jy when $\sigma_{\rm c}$ changes from zero to $2.44\,\mu$Jy beam^{-1} and verify that the integration time τ needed to reach the new value of $\sigma_{\rm n}$ agrees with the Time on Source calculated by the VLA Exposure Calculator.

[If you leave *RMS Noise (units/beam)* = 10 μJy and change the *Array Configuration* to D (maximum baseline $\approx$ 1 km), you will see that the *RMS Noise (units/beam)* jumps to 25.8 μJy, and you should get a warning message that the rms confusion is 25.8 μJy beam^{-1}. Confusion makes it impossible to reach 10 μJy beam^{-1} rms with the D configuration at S band, no matter how long the integration time.]

Problem Set 8

25. (20 points) Hot supergiant stars, such as the bright blue star Rigel A in the constellation Orion, can shed mass at rates $\dot{M} \approx 10^{-5} M_\odot \text{ yr}^{-1}$ via ionized stellar winds. Consider a spherical, isothermal (at temperature $T \approx 10^4$ K), and fully ionized pure hydrogen wind starting at the photospheric radius $r_0 \approx 7 \times 10^{12}$ cm and flowing radially outward with constant velocity $v \approx 300 \text{ km s}^{-1}$ to a distance $\gg r_0$.

    (a) (4 points) What is the electron density N_0 at the base of the wind just above the photosphere of Rigel?

    (b) (4 points) What is the ionized wind emission measure EM in pc cm^{-6} along a radial line of sight from the photosphere to a distant observer?

    (c) (4 points) What is the ionized wind optical depth τ_ν along this line of sight at $\nu = 10$ GHz?

    (d) (4 points) Because the ionized wind optical depth is $\tau_\nu \gg 1$ at $\nu = 10$ GHz, the photosphere of Rigel A is buried and radio astronomers can see only the wind from the star. The opacity coefficient is declining rapidly with r (you can easily show that $\kappa_\nu \propto r^{-4}$), so we will make the simple approximation that the wind looks like a black body whose radius $r_{\rm bb}$ is about equal to the radius at which $\tau \approx 1$. Show that $r_{\rm bb}$ is proportional to $\nu^{-0.7}$.

    (e) (4 points) Show that the flux density of the wind is proportional to $\nu^{+0.6}$ at radio frequencies.

Problem Set 9

26. (5 points) White dwarf stars are the cores remaining after low-mass stars have expelled most of their outer layers during the red giant phase. They typically have masses $M \sim M_\odot$ and radii $r \sim 10^4$ km comparable with the radius of the Earth ($r_\oplus \approx 6.5 \times 10^3$ km). They are nearly black bodies with surface temperatures high enough to ionize hydrogen and light up planetary nebulae. Show that even the hottest white dwarfs cannot maintain surface temperatures $T > 10^6$ K.

27. (5 points) Measurements of the stronger ($S \gtrsim 1$ Jy) extragalactic synchrotron sources have shown that many have brightness temperatures as high as $T_B \sim 10^{11}$ K at radio wavelengths. Approximately what size radio telescope is needed to resolve such sources at any radio wavelength?

28. (5 points) Estimate the typical Lorentz factor γ of electrons emitting synchrotron radiation at $\nu = 1.4$ GHz in the $B \sim 5\ \mu$G interstellar magnetic field of our Galaxy.

29. (5 points) The synchrotron lifetime τ_s of a radio source is defined as ratio of its total electron energy E_e to the average synchrotron power $\langle P \rangle$ emitted by the electrons in a magnetic field of strength B. Derive an equation for the synchrotron lifetime of just those electrons with critical frequency $\nu_\mathrm{c} = 1.4$ GHz in the $B = 5\,\mu$G interstellar magnetic field of our Galaxy, and estimate their synchrotron lifetime in years.

Problem Set 10

30. (20 points) The far-infrared (FIR) luminosity of a star-forming galaxy is proportional to its recent star-formation rate. The 1.4 GHz radio luminosities of most star-forming galaxies are observed to be nearly proportional to their FIR luminosities. This is the famous FIR/radio correlation that makes the radio luminosity a useful measure of the recent star-formation rate. Most of the 1.4 GHz radio luminosity is synchrotron radiation from relativistic electrons that were accelerated in the supernova remnants of massive, short-lived stars, so it makes sense that the number of relativistic electrons would be proportional to the recent star-formation rate. Thus the tight FIR/radio correlation seems to require that a fixed fraction of the energy in these relativistic electrons be turned into radio radiation.

    However, every relativistic electron that emits synchrotron radio emission also loses energy by inverse-Compton (IC) scattering, which converts electron energy into ultraviolet or X-ray emission. In the "calorimeter" model for the FIR/radio correlation, relativistic electron energy is lost through two channels: synchrotron radiation and IC radiation. Thus excessive IC scattering might reduce the synchrotron emission and cause the FIR/radio correlation to break down.

    (a) (4 points) Consider a simple model in which the relativistic electrons in nearby star-forming galaxies lose energy only by synchrotron radiation and by IC scattering off the $T = 2.73$ K blackbody cosmic microwave background (CMB) radiation that fills the universe. What is the minimum magnetic field strength $B_{\rm min}$ in a nearby galaxy such that the IC losses do not exceed the synchrotron losses?

    (b) (4 points) Show that the fraction f of the relativistic electron energy going into synchrotron radiation is fairly constant when $B > B_{\rm min}$, which is consistent with the FIR/radio correlation, but drops rapidly for $B < B_{\rm min}$, which is not consistent with the FIR/radio correlation.

    (c) (4 points) Most nearby spiral galaxies have magnetic field strengths $B \sim 5\ \mu$G. Should they obey the FIR/radio correlation? In the distant past at redshift z, the temperature of the CMB radiation was $(1+z) \cdot 2.73$ K. Should we expect galaxies with $B \sim 5\ \mu$G to obey the FIR/radio correlation at $z = 2$?

    (d) (4 points) ULIRGs are Ultra-Luminous InfraRed Galaxies, most of which contain extremely luminous (bolometric luminosity $L \sim 10^{11.5} L_\odot$) compact (radius $R \sim 100$ pc) starbursts. The energy density $U_{\rm rad}$ of starlight in ULIRGs greatly exceeds the energy density of the CMB radiation. Show that $U_{\rm rad} \sim 10^{-7}$ erg cm^{-3} in ULIRGs.

    (e) (4 points) Despite their high radiation energy densities, ULIRGs still obey the FIR/radio correlation. Estimate the minimum magnetic field strength $B_{\rm min}$ such that $U_{\rm bmin} = U_{\rm rad}$ in ULIRGs.

Problem Set 11

31. (6 points) The frequency-dependent delays shown in *ERA* Figure 6.5 are due to dispersion by the ionized interstellar medium in our Galaxy, whose electron density is $n_{\rm e} \sim 0.03\,{\rm cm}^{-3}$. The frequency range plotted extends from $\nu_{\rm lo} = 300\,{\rm MHz}$ to $\nu_{\rm hi} = 395\,{\rm MHz}$.
    (a) (3 points) If that pulsar has a spin period $P = 1.2\,{\rm s}$, what is the Dispersion Measure (DM) towards the pulsar?
    (b) (1 point) What is the rough distance to the pulsar?
    (c) (2 points) If we are conducting a pulsar survey using the same receiver that provided the data for Figure 6.5, approximately what would the stepsize in DM be if we didn't want an error in DM to smear our signal more than $100\,\mu{\rm s}$ in order to detect millisecond pulsars (MSPs)? Roughly how many independent DMs would we have to search if we wanted to search to a maximum DM of $100\,{\rm pc\,cm}^{-3}$?

32. (6 points) When it was realized that pulsars appear to be slowing down with time (i.e., $\dot{P} > 0$), one of the explanations was a second-order effect that would result if the pulsars had a large transverse velocity component V in the plane of the sky (Shklovskii, I. S. 1970, Soviet Astron., AJ, 13, 562).
    (a) (4 points) If all of the pulsar's measured spin-down is due to the "Shklovskii effect" and the pulsar is at a distance d, show that
    $$\dot{P}_{\rm S} = \frac{V^2}{dc} P \ .$$
    (b) (2 points) Using the P$\dot{\rm P}$ diagram (*ERA* Figure 6.3), and assuming a typical $V = 200\,{\rm km\,s}^{-1}$ and typical distances between 0.1 kpc and 10 kpc, does the Shklovskii effect contribute significantly ($\dot{P}_{\rm S} > 0.01\dot{P}$), for instance, to the observed $\dot{P}$ of any pulsars? If so, which ones?

33. (11 points) You have recently found an interesting X-ray point source with *Chandra* which you suspect is a pulsar. You point the GBT at it and discover an isolated pulsar with a spin period of 0.0840035907(1) seconds based on your discovery observation. Since you already have a precise position from the X-ray observation, you immediately request timing observations over the next couple weeks with the hope of measuring the spin-down rate and the associated physical parameters of the pulsar based on it. The first two TOAs below are from your discovery observation. Here are the arrival times in MJD from the GBT after correcting them to the Solar System barycenter (i.e. to remove the effect of the Earth's motion). The errors on each are about 0.3 ms.

MJD
54888.5315263508382
54888.7833601709499
54889.6818806806114
54891.8215009488777
54895.0038998945965
54900.7409878392282

You can download these from `https://www.cv.nrao.edu/~sransom/ps10_TOAs.txt`

    (a) (2 points) Given the total time baseline between first TOA and last, as well as the approximate TOA uncertainties, estimate the precision with which you should be able to measure the spin frequency ν and the spin frequency derivative $\dot{\nu}$. For this example, because of the small number of TOAs and the covariances between ν and $\dot{\nu}$, you will not be able to do quite that well.
    (b) (6 points) Determine ν and $\dot{\nu}$ (referenced to the time of the first TOA) using a timing analysis of your choosing that properly accounts for all the rotations of the pulsar. Counting the first TOA as rotation zero, record the rotation numbers of the pulsar for each TOA. **Hint: You should only add a single TOA at a time (i.e. iterate or re-do the "solution" each time, using the previous answers as your new starting points)) while you are determining your solution or you may mis-count the pulse numbers!** Alternatively, you could try a brute force solution

since you know that there are an integer number of rotations between each pulse. Make sure that you include your code (or at least a good description of what you did) for this part. Remember that since the TOA errors are about 0.3 ms each, the resulting model should predict each of their phases to approximately that precision! If that is not the case when you have a final answer, then you do not have a good timing solution!

(c) (3 points) Estimate the $\dot{E}$, magnetic field strength, and characteristic age τ of the pulsar. What kind of a pulsar is this?

Problem Set 12

34. (8 points) The recent paper "HII region ionization of the interstellar medium: a case study of NGC 7538" by Metteo Luisi, L. D. Anderson, Dana S. Balser, T. M. Bania, & [UVa astronomy grad student] Trey V. Wenger 2016, ApJ, 824, 125 includes a GBT recombination-line spectrum (Figure 1) at position W2 in the HII region NGC 7538. It is the aligned average of the seven transitions (87α through 93α) observed simultaneously at seven frequencies from 9.812 to 8.046 GHz. The observed radial velocity of the hydrogen line center is $v_\mathrm{r} = -60$ km s^{-1}. The ^{12}C carbon line and the ^{4}He helium line are at the same radial velocity, but they appear at more negative velocities on the plot because these lines have higher rest frequencies. The fitted Gaussians have peak antenna temperatures $T_\mathrm{A} = 181.2$ mK (H) and 21.7 mK (He), and full widths between half-maximum points (FWHMs) $\Delta v_r = 24.6$ km s^{-1} (H) and 18.6 km s^{-1} (He). The lines are optically thin.

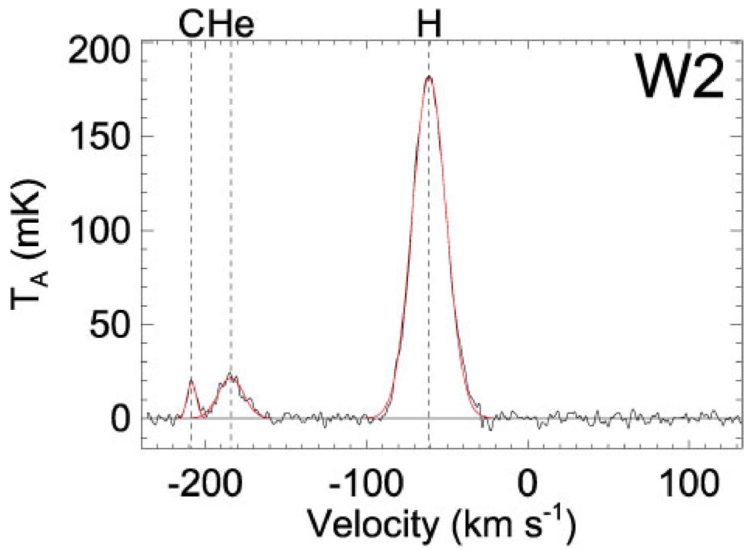

Figure 1: The recombination-line spectrum at position W2 in the HII region NGC 7538 with Gaussian fits (red) to the H, He, and C lines. The velocity scale indicates the radial velocity relative the the rest frequency for the H line.

(a) (4 points) Calculate the velocity at which the dotted line indicating the center of the He line should be plotted in Figure 1. [Tip: Use the approximations $M_\mathrm{H} = 1.67 \times 10^{-24}$ g and $M_\mathrm{He} = 4M_\mathrm{H}$ for simplicity; your result will still be quite accurate.]

(b) (4 points) About how many He$^+$ ions are there per H$^+$ ion?

35. (12 points) Rotating polarized molecules emit radio-frequency spectral lines that can penetrate dusty molecular clouds and reveal physical conditions such as density and temperature in the obscured regions where most new stars are born in our own Galaxy, in nearby galaxies, and even in the luminous star-forming galaxies at high redshifts that account for the bulk of star formation in the universe (Carilli & Walter 2013, ARA&A, 51, 105). The ^{12}C^{16}O isotope of carbon monoxide is the most abundant and universal radio tracer of diffuse interstellar molecular gas, and HCN (hydrogen cyanide) is especially useful for pinpointing the densest gas ($n > 10^5$ cm^{-3}) that is about to form stars (Gao & Solomon 2004, ApJ, 606, 271).

The critical number density n^* (cm^{-3}) of molecules (*ERA* Equation 7.135) is the minimum density needed for collisions to bring the molecular excitation temperature close to the gas kinetic temperature, so strong lines are emitted only by regions with densities $n \approx n(\mathrm{H}_2) \gtrsim n^*$. The critical density depends both on the emitting molecular species (e.g., CO, HCN, ...) and on the upper rotational quantum number J, so different lines from different species respond to regions with different densities.

Similarly, there is a minimum gas temperature $T_{min} \sim E_{\rm rot}/k$ below which most collisions are insufficiently energetic to excite the upper-level rotational quantum number J of a particular rotational line (*ERA* Section 7.7.2).

Panel "a" shows how increasing $\log(n)$ increases higher-J CO emission from gas with fixed temperature $T = 40$ K. Panel "b" shows how increasing the gas temperature increases higher-J CO emission from gas with fixed density $\log(n) = 3.4$.

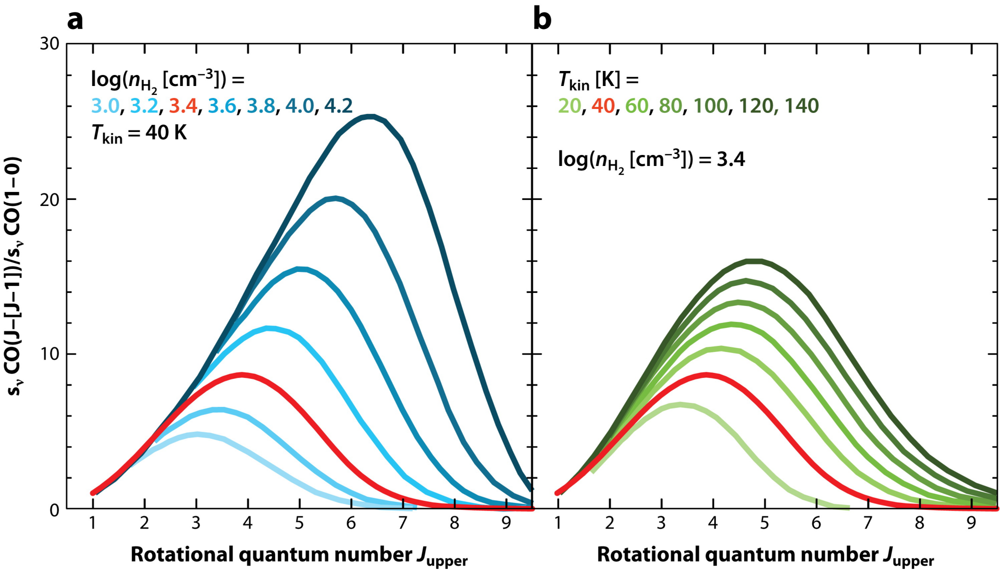

Carilli CL, Walter F. 2013.
Annu. Rev. Astron. Astrophys. 51:105–61

(a) (4 points) Show that the critical density n^* at which the collisional excitation rate balances the radiative deexcitation rate for the $J \to J-1$ rotational transition is

$$n^* \propto \frac{3J^4}{2J+1}$$

times the critical density of the $J = 1 \to 0$ transition. Thus higher densities are needed to excite lines with higher J, as shown in Panel "a." Note that this result applies to all species of linear rotating molecules, not just CO.

(b) (4 points) *ERA* Equation 7.133 gives the spontaneous emission rate for the $J \to J-1$ rotational transition as

$$\left(\frac{A_{J\to J-1}}{\rm s^{-1}}\right) \approx 1.165 \times 10^{-11} \left|\frac{\mu}{\rm D}\right|^2 \left(\frac{J}{2J+1}\right)\left(\frac{\nu}{\rm GHz}\right)^3 ,$$

where $\mu/{\rm D}$ is the electric dipole moment in units of Debye $= 10^{-18}$ statcoul cm. The dipole moment of the common CO molecule is only $\mu \approx 0.11$ D, but some molecules have much higher dipole moments. In particular, the HCN (hydrogen cyanide) molecule has $\mu \approx 2.7$ D. The measured rest frequency of the HCN $J = 1 \to 0$ line is $\nu \approx 88.6$ GHz. Compare the critical density of the HCN $J = 1 \to 0$ transition with that of the CO $J = 1 \to 0$ transition, $n^* \approx 1.4 \times 10^3$ cm^{-3}.

(c) (4 points) Fill in the table below with CO and HCN critical densities for lines with upper rotational quantum numbers $J = 1$, 2, 3, and 4 by scaling from the value $n^* = 1.4 \times 10^3$ cm^{-3} for the $J = 1 \to 0$ CO line.

$J \to J-1$	n^*(CO) (cm^{-3})	n^*(HCN) (cm^{-3})
$J = 1 \to 0$	1.4×10^3	?
$J = 2 \to 1$	?	?
$J = 3 \to 2$	?	?
$J = 4 \to 3$	?	?